Research Article

MOLECULAR PAIN

Molecular Pain
Volume 20: 1–15

DOI: 10.1177/17448069231225810
journals.sagepub.com/home/mpx
Sage

Kilohertz high-frequency electrical stimulation ameliorate hyperalgesia by modulating transient receptor potential vanilloid-1 and N-methyl-D-aspartate receptor-2B signaling pathways in chronic constriction injury of sciatic nerve mice

Kexin Fang[1,2], Peixin Lu[1,2], Wen Cheng[1,2], and Bin Yu[1,2]

Abstract

The number of patients with neuropathic pain is increasing in recent years, but drug treatments for neuropathic pain have a low success rate and often come with significant side effects. Consequently, the development of innovative therapeutic strategies has become an urgent necessity. Kilohertz High Frequency Electrical Stimulation (KHES) offers pain relief without inducing paresthesia. However, the specific therapeutic effects of KHES on neuropathic pain and its underlying mechanisms remain ambiguous, warranting further investigation. In our previous study, we utilized the Gene Expression Omnibus (GEO) database to identify datasets related to neuropathic pain mice. The majority of the identified pathways were found to be associated with inflammatory responses. From these pathways, we selected the transient receptor potential vanilloid-1 (TRPV1) and N-methyl-D-aspartate receptor-2B (NMDAR2B) pathway for further exploration. Mice were randomly divided into four groups: a Sham group, a Sham/KHES group, a chronic constriction injury of the sciatic nerve (CCI) group, and a CCI/KHES stimulation group. KHES administered 30 min every day for 1 week. We evaluated the paw withdrawal threshold (PWT) and thermal withdrawal latency (TWL). The expression of TRPV1 and NMDAR2B in the spinal cord were analyzed using quantitative reverse-transcriptase polymerase chain reaction, Western blot, and immunofluorescence assay. KHES significantly alleviated the mechanical and thermal allodynia in neuropathic pain mice. KHES effectively suppressed the expression of TRPV1 and NMDAR2B, consequently inhibiting the activation of glial fibrillary acidic protein (GFAP) and ionized calcium binding adapter molecule 1 (IBA1) in the spinal cord. The administration of the TRPV1 pathway activator partially reversed the antinociceptive effects of KHES, while the TRPV1 pathway inhibitor achieved analgesic effects similar to KHES. KHES inhibited the activation of spinal dorsal horn glial cells, especially astrocytes and microglia, by inhibiting the activation of the TRPV1/NMDAR2B signaling pathway, ultimately alleviating neuropathic pain.

Keywords

Kilohertz frequency electrical stimulation, neuropathic pain, spinal glial cells, the transient receptor potential vanilloid-1/N-methyl-D-aspartate receptor-2B pathway

Date Received: 16 September 2023; Revised 30 November 2023; accepted: 12 December 2023

[1]Department of Anesthesia and Pain Rehabilitation, Yangzhi Affiliated Rehabilitation Hospital of Tongji University, Shanghai, China
[2]Tongji University School of Medicine, Shanghai, China

Corresponding Author:
Bin Yu, Department of Anesthesia and Pain Rehabilitation, Yangzhi Rehabilitation Hospital Affiliated to Tongji University School of Medicine, 2209 Guangxing Road, Songjiang District, Shanghai 200092, China.
Email: yubin@tongji.edu.cn

Introduction

Neuropathic pain has been redefined by the International Association for the Study of Pain as pain caused by damage or disease of the somatosensory system.[1] Approximately 7% to 10% of the general population suffer from neuropathic pain.[2] Patients primarily exhibit hyperalgesia, allodynia, and spontaneous pain.[3] The pathogenesis involves ectopic activity, peripheral and central sensitization, impaired inhibitory modulation, and pathological activation of glial cells.[4] In clinical practice, first-line pharmacological treatments for neuropathic pain include local anesthetics, tricyclic antidepressants, and anticonvulsants, but these drugs are effective in less than 50% of patients.[5] Clinically, researchers are continuously exploring effective physical therapies, among which KHES ranging from 1 kHz to 100 kHz provides pain relief without causing paresthesia.[6] The KHES device comprises a high-frequency electrical stimulation generator and corresponding needle electrodes, offering advantages such as immediacy, minimally invasive nature, selectivity, and controllability.[7] Although there have been some studies on treating neuropathic pain by KHES,[5] the underlying mechanism remains in the hypothetical stage.

In our previous study, we identified suitable datasets for neuropathic pain mice (GSE60670, GSE123919, GSE111216, and GSE117320) from the publicly available GEO database. Subsequent Kyoto Encyclopedia of Genes and Genomes (KEGG) pathway analysis revealed key signaling pathways, including the nuclear factor κB (NF-κB) pathway, glutamatergic synapse, inflammation-mediated transient receptor potential (TRP) channels, and cyclic adenosine monophosphate (cAMP) signaling pathway (Supplementary Figure 1). Notably, it has been demonstrated that the myeloid differentiation factor 88 (Myd88) and NF-κB signaling pathway play significant roles in the process of KHES-mediated inhibition of neuropathic pain.[8] Glutamatergic synapse and TRP channels, known as ion channels involved in sensory transmission, are also considered potential pathways implicated in the development of neuropathic pain.[8] Glutamate, an essential neurotransmitter in the mammalian central nervous system, plays an irreplaceable role in pain perception and subsequent signal transduction.[9,10] Among them, N-methyl-D-aspartate (NMDA) and its receptors are responsible for transmitting spinal cord injury information.[11] Studies have shown the involvement of NMDAR2B receptors in the activation of spinal dorsal horn glial cells in neuropathic pain models.[12] TRPV1, a member of the transient receptor potential (TRP) channel family, is widely expressed in primary sensory neurons and has been implicated in the transmission and modulation of pain signals. Previous studies have shown TRPV1 is present in small- and medium-sized DRG neurons, in spinal laminas I and II inner and in sciatic nerve.[13] Mruvil Abooj et al. found a significant increase in the expression of TRPV1 in the central sensory nerve terminals that form synapses with the second order neurons in the CCI model.[14] It has been proved an upregulation of TRPV1 expression in the dorsal root as well as the entry area in the spinal dorsal horn in animal models of neuropathic pain, indicating its potential involvement in the pathophysiology of this condition.[15–17] As a selective proton-sensitive cation channel, TRPV1 can be effectively blocked by the TRPV1 channel antagonist capsaicin,[18,19] while its activation can be facilitated by the activator SB-705498.[20,21] It has been confirmed that the TRPV1 channel contributes to remifentanil-induced postoperative hyperalgesia by regulating NMDA receptor trafficking in the dorsal root ganglions.[22] Additionally, the activation of TRPV1 triggers downstream activation of glial cells, including microglia and astrocytes,[23,24] which significantly contribute to the development and maintenance of neuropathic pain. Building on previous research findings and bioinformatics analysis, this study focused on exploring the TRPV1/NMDAR2B pathway in the process of KHES analgesia.

Material and methods

Experimental animals

80 adult male C57BL/6 mice, aged 7–8 weeks and weighing 20–30 g, were purchased from Shanghai SLAC Laboratory Animal Co. Ltd [License No. SCXK (Shanghai) 2013-0006]. The mice were housed alone in a climate-controlled chamber with a 12/12 h light/dark cycle and provided with adequate food and water. All experiments were conducted at Shanghai Tongji Hospital following the ethical code of experimental animals. The methods were performed under the relevant guidelines and regulations of the International Association for the Study of Pain.

Chronic constriction injury model

The mice were randomly divided into four groups: a Sham group, a Sham/KHES group, a CCI group, and a CCI/KHES stimulation group. After administering 0.8% pentobarbital sodium anesthesia, the surgical area was disinfected with 75% alcohol. The skin was dissected longitudinally above the lateral femur, and the muscle was bluntly separated along the muscle striae. The sciatic nerve was exposed, and the surrounding tissue was dissociated. A polyethylene 90 tube (Outside diameter, 0.6 mm; Inner diameter, 0.3 mm) was ligated to the sciatic nerve.[25,26] The cannula was gently pressed to allow for slight muscle twitching. The mice in the Sham group were dissected according to the CCI modeling procedure, but the sciatic nerve was not treated. To determine whether the modeling was successful, we observed the gait, hind limb posture, local skin, and muscle tension of the mouse every 1–2 days after the operation.

Kilohertz high frequency electrical stimulation stimulation parameters

Firstly, we need to determine the motor threshold (MoT) of mice, which is determined by gradually increasing the current intensity of electrical stimulation. The current intensity is increased from zero until muscle contractions are observed in the lower mid-trunk or hind limbs, at which point the current intensity is considered as the MoT. The sensory threshold (SenT) refers to the level of stimulus intensity that causes the animal to shift attention or slightly adjust body posture to adapt to the stimulus. According to recent research, we found that the SenT of mice is approximately close to 50% of the MoT.[27,28] Employing an electrical stimulation intensity of 40% MoT is considered an appropriate approach for alleviating animal pain.[29] Therefore, we adopted this method as a reference in our study.

After anesthesia with 2% isoflurane, the mice were fixed on a platform in the right lateral recumbent position. Following shaving of the mouse's fur and disinfection of the puncture site with alcohol, a sterile needle electrode was inserted to a depth of approximately 3 mm. The sciatic nerve in the mouse was electrically stimulated using a needle electrode with dimensions of 0.3 mm in diameter and 13 mm in length. The stimulating electrode was placed at a distance of 2–5 mm from the CCI model at the distal end of the sciatic nerve. The recording electrode was placed in the tibialis anterior muscle belly, and a needle-like high-frequency stimulation electrode was positioned between the stimulation electrode and the recording electrode. The reference electrode was placed in the tibialis anterior tendon, and the ground electrode was placed in the mouse's tail. The sciatic nerve compound muscle action potential (CMAP) of the Sham/KHES and the CCI/KHES stimulation groups was measured using a nerve-evoked potentiometer and electrophysiological monitor (Nuocheng Co., China). The stimulus program interface and stimulus parameters were shown in Figure 2. The stimulation frequency range was adjusted to 17–20 kHz, and the electrical current intensity was slowly increased until muscle contractions in the mouse's hind limbs were observed, at which point the CMAP was recorded. This current intensity represented the MoT of the mouse's sciatic nerve. Finally, an intensity of 40% of the MoT was employed as the current intensity for KHES. Electrical stimulation was administered from Day 7 to Day 13 after modeling. The sham group underwent the same procedure for inserting needle electrodes and received concurrent electrical stimulation. The entire experimental protocol was conducted in accordance with the illustration in Figure 1.

Behavioral studies

The mechanical pain threshold in mice was evaluated by measuring the PWT. The mice were placed on a wire mesh grid and covered with a transparent acrylic glass box for 30 min to acclimate them. After a 3-day adaptation period in the environment, the mice were tested using Von Frey filaments of different intensities (0.04, 0.07, 0.16, 0.4, 1, 1.4, and 2 g). These filaments were vertically applied to the mice's hind paws near the plantar region, with a stimulation time not exceeding 5 s. Five consecutive stimulations were performed, with a minimum interval of 30 s between each pair of stimulations, and the mice's responses were recorded. A positive response was recorded when the mice exhibited paw withdrawal or licking. If there were at least three positive responses out of five stimulations, the next lower intensity Von Frey filament was used. Otherwise, the next higher intensity filament was employed. Finally, the non-parametric Dixon test method was utilized to record the PWT in mice.[30] The TWL in mice was measured to assess their thermal pain threshold.[31] The mice were placed on a glass plate and covered with a transparent acrylic glass box for 1 h to adapt them. After a 3-day adaptation period in the environment, the mice were tested using a thermal pain stimulation device (Shanghai Yuyan Instrument Co., Ltd). The mice were placed on a glass plate with a laser beam being used to illuminate their paws. The laser emitter was located at 0.5 cm from the bottom of the mice's paws, and the cut-off time was set to 20 s to prevent tissue damage. When the mice showed a paw withdrawal or licking, the laser was shut down and the time was recorded simultaneously. The average time of the three stimulations was used as the TWL of the mice, and there was a minimum interval of 10 min between each stimulation. The mechanical and thermal pain threshold tests were conducted 1 hour after KHES from Day7 to Day13 (Figure 1). At this time point, the mice, which were anesthetized with 2% isoflurane, had fully recovered to a conscious state, ensuring the test results were not affected.

According to the experimental procedure shown in Figure 1, we conducted rotarod test and open field and experiments on mice before and after modeling, as well as on Day13. The motor coordination ability of the mice was evaluated using a mouse rotary rod instrument (Shanghai Yuyan Instruments Co., Ltd). The mice were placed on a rotating rod with a diameter of 3 cm, and the rotation speed was adjusted to 30 r/min. Five mice were measured at the same time, and the time to fall from the rods was recorded using the same parameters. The stopping time was set as 5 min. Additionally, the open-field test was used to assess motor function. The inner walls and bottom surface of the square box were cleaned to prevent residual information from the previous mouse. The mouse was placed in the bottom center of the box, and the video and time were recorded simultaneously. The camera stopped after 10 min of observation, and the moving distance and speed of the mouse were recorded.

Drug administration

To activate TRPV1, we administered the TRPV1 activator capsaicin (HY-10488; MedChem Express, Shanghai, China)

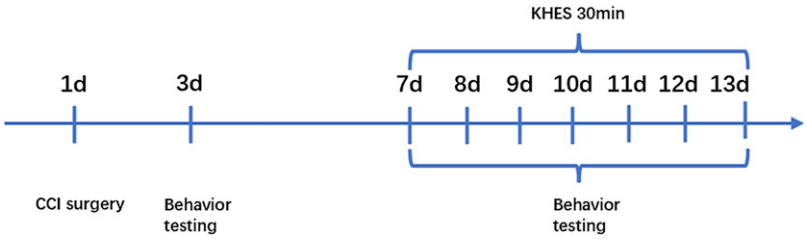

Figure 1. Experimental design schedule. CCI surgery was conducted on Day 1. KHES was administrated from day 7 to day 13. Behavior tests were conducted on day 3, day 7, day 8, day 9, day 10, day 11, day 12, and day 13. Mice were euthanized, and their spinal cords were obtained after a 13-day experiment.

intraperitoneally at a concentration of 10 mg/kg 1 hour prior to KHES on Day 7.[32] Conversely, to inhibit TRPV1, we administered the inhibitor SB-705498 (HY10633; MedChem Express, Shanghai, China) orally at a concentration of 10 mg/kg on Day 7.[33] In both cases, we used 20% dimethyl sulfoxide as the vehicle.

Western blotting

After the 13-Day experiment, all mice were anesthetized with 2% isoflurane, and the right side of lumbar 4–6 spinal cord was harvested. Total protein was extracted with Radio-Immunoprecipitation Assay (RIPA) buffer. Proteins were separated by sodium dodecyl sulphate-polyacrylamide gel electrophoresis (SDS-PAGE) on 7.5%, 10%, or 15% gels and transferred to polyvinylidene fluoride (PVDF) membranes. The membranes were incubated in blocking buffer (5% skim milk) for 2 h before being incubated overnight at 4°C with primary antibodies, including TRPV1 (1:3000, 66983-1-Ig, Proteintech Group, Inc.), NMDAR2B (1:1000, D8E10, Cell Signaling Technology, Inc.), IBA-1 (1:1000, AB5076, Abcam, Inc.), GFAP (1:500, G6171, Sigma, Inc.), β-actin (1:1500, D6A8, Cell Signaling Technology, Inc.), and GAPDH (1:1500, D16H11, Cell Signaling Technology, Inc.). The membranes were washed three times with Tris-Buffered Saline and Tween-20 (TBST) for 10 min each and then incubated with secondary antibodies, such as horseradish peroxidase (HRP)-conjugated AffiniPure goat anti-rabbit IgG (1:5000, Cat. No. SA00001-2, Proteintech Group, Inc.) and HRP-conjugated AffiniPure goat anti-mouse IgG (1:5000, Cat. No. SA00001-1, Proteintech Group, Inc.). Finally, the bands were visualized using Enhanced Chemiluminescence (ECL) substrates, and the intensity analysis was conducted using ImageJ software.

Immunofluorescence

The mice in the four groups were anesthetized with 2% isoflurane. A solution of 0.9% saline and 4% paraformaldehyde was used to perfuse the mice. The L4-L6 spinal cord was removed and fixed. 25 μM spinal cord sections were cut on a cryo-thermostat for immunofluorescence staining. After rinsing with phosphate-buffered normal saline (PBS), sections were permeated with 0.3% Triton X-100. They were then sealed with 10% normal goat serum for 2 h and incubated with primary antibodies overnight. The primary antibody markers were TRPV1(1:300, Proteintech Group, Mouse, No. 66983-1-Ig.), NMDAR2B (1:100; Abcam, Rabbit. No. Ab565783), Ionized calcium-binding adapter molecule 1 (IBA-1;1:200; Abcam, Goat. No. Ab5076), and glial fibrillary acidic protein (GFAP; 1:200; Sigma, Mouse. No. G6171). 4,6-diamino-2-phenyl indole (DAPI; 5 μg/ml; Sigma- Aldrich) was used to label the nuclei. The sections were then incubated for 2 h with Alexa Fluor 350 and 488 secondary antibodies. Finally, images were captured using a Zeiss LSM510 confocal microscope (Zeiss, Thornwood, CA, USA).

Quantitative reverse-transcriptase polymerase chain reaction (qPCR)

The L4-L6 spinal dorsal horn was collected for qPCR analysis. Total RNA was extracted using the TRIzol method. We used oligo-DT primers (Sangon Biotech Co., Ltd, China) to perform reverse transcription. Each sample was divided into three replicates, with 20 μL for each replicate, including 10 μM for forward and reverse primers, 10 μL for SYBR Green qPCR Super Mix (Invitrogen), and 25 ng cDNA. The reaction was carried out in an Applied Biosystems 7500 rapid real-time PCR system. The 2-DDCt method was used to determine the relative expression levels of TRPV1, NMDAR2B, IBA-1, GFAP, and GAPDH mRNA in the spinal cord tissue. The sequences of murine-specific primers used to detect TRPV1, NMDAR2B, IBA-1, GFAP, and GAPDH mRNA are listed in Table 1, and the primers were obtained from Sangon.

Statistical analyses

The data were expressed as mean ± SEM, and statistical analysis was performed using SPSS 22.0 statistical software. One-way ANOVA was conducted, followed by Tukey post hoc tests for comparisons between multiple groups. A p-value less than 0.05 was considered statistically significant.

Table 1. Sequences (5′-3′) of primers used in qPCR.

Gene	Forward primer	Reverse primer
TRPV1	AGCAGCAGTGAGACCCCTAAC	CAAGCAGTAGACGAAGAAGTTGA
NMDAR2B	GCCATGAACGAGACTGACCC	GCTTCCTGGTCCGTGTCATC
GFAP	CGGAGACGCATCACCTCTG	TGGAGGAGTCATTCGAGACAA
Iba-1	ATCAACAAGCAATTCCTCGATGA	CAGCATTCGCTTCAAGGACATA
GAPDH	AATGGATTTGGACGCATTGGT	TTTGCACTGGTACGTGTTGAT

Results

Determination of the kilohertz high frequency electrical stimulation parameters

The CCI/KHES and Sham/KHES groups were subjected to high-frequency electrical stimulation at 15–20 kHz for 30 min per day for 7 days, starting from Day 7 to Day 13. The electrode placement is depicted in Figure 2(a). The electrical stimulation employed a gradually increasing current intensity to determine the MoT of the mouse sciatic nerve. Starting from 0.2 mA, the contraction of the hind limb muscles in mice was observed. The results indicated that when the current intensity was adjusted to 1.2 mA, there was a noticeable contraction in the mouse muscles, and further increasing the current intensity did not result in significant changes in the contractions. As shown in Figure 2(b), the CMAP exhibited a typical waveform at this current intensity, and increasing the current did not lead to an increase in its amplitude. Therefore, we determined the MoT of the mouse sciatic nerve in this experiment to be 1.2 mA, with an intensity of approximately 40% of that being around 0.5 mA. After determining the stimulation current, we performed electrical stimulation at different frequencies and found that the best blocking effect of KHES occurred at frequencies between 17 and 19 kHz (Figure 2(c)). In subsequent KHES experiments, we applied the stimulation mode using a frequency of 17–19 kHz and an intensity of 0.5 mA.

Kilohertz high frequency electrical stimulation improved neuropathic pain without affecting motor function

On Day 3 and Day 7, PWT and PWL of the CCI group were significantly lower than those of the sham group, indicating the successful modeling of modified CCI mice (Figure 3(a), $p < .001$; Figure 3(b), $p < .05$). From Day 7 to Day 13, the CCI/KHES and Sham/KHES groups were subjected to high-frequency electrical stimulation of the sciatic nerve on the operative side. During the 30 min of electrical stimulation, 2% isoflurane gas anesthesia was administered, and the mice regained consciousness approximately 0.5 h after KHES stimulation. PWT was measured 1 h after the end of the stimulation, and the duration of analgesia was monitored. The antinociceptive durations of KHES for mechanical allodynia were 2 h on Day 7 (Figure 4(a), $p < .0001$ for 2 h), 2 h on Day 8 (Figure 4(b), $p < .0001$ for 2 h), 3 h on Day 9 (Figure 4(c), $p < .01$ for 3 h), 5 h on Day 10 (Figure 4(d), $p < .05$ for 5 h), 5 h on Day 11 (Figure 4(e), $p < .05$ for 5 h), 6 h on Day 12 (Figure 4(F), $p < .05$ for 6 h), and 6 h on Day 13 (Figure 4(G), $p < .05$ for 6 h). The results indicated that the analgesic duration of the CCI model mice increased with an increase in the number of days of high-frequency electrical stimulation, up to 6 h, which demonstrated the feasibility of high-frequency electrical stimulation in treating neuropathological pain from the perspective of behavior. Moreover, there was no change in rod rotation (Figure 3(c), $p > .05$) and open-field test (Figure 3(d)–(e), $p > .05$) in CCI mice before and after KHES stimulation, indicating that KHES stimulation did not affect motor function.

Kilohertz high frequency electrical stimulation inhibited the expression of transient receptor potential vanilloid-1 and N-methyl-D-aspartate receptor-2B in the spinal cord

To investigate the potential mechanisms underlying the analgesic effects of KHES in CCI mice, we examined the modulation of the TRPV1/NMDAR2B signaling pathway. We utilized Western blot analysis to assess the protein expression of TRPV1 and NMDAR2B in the spinal cord. The results showed a significant increase in the expression of TRPV1 and NMDAR2B in the CCI group compared to the sham group (Figure 5(a)–(d), $p < .001$ for TRPV1; $p < .001$ for NMDAR2B). However, KHES treatment effectively reversed the upregulation of TRPV1 and NMDAR2B in CCI mice ((Figure 5(a)–(d), $p < .01$ for TRPV1; $p < .001$ for NMDAR2B)). Notably, the Sham/KHES group did not exhibit any significant changes in the protein expression of TRPV1 and NMDAR2B compared to the Sham group (Figure 5(a)–(d)). Furthermore, we assessed the mRNA levels of TRPV1 and NMDAR2B in the spinal cord using QPCR. The results showed that the activation and mRNA expression of TRPV1 and NMDAR2B were significantly upregulated in the CCI group compared to the Sham group (Figure 5(e)–(f), $p < .0001$ for TRPV1; $p < .0001$ for NMDAR2B). However, KHES treatment significantly inhibited the mRNA expression of TRPV1 and NMDAR2B (Figure 5(e)–(f), $p < .0001$ for TRPV1; $p < .0001$ for NMDAR2B). To further confirm

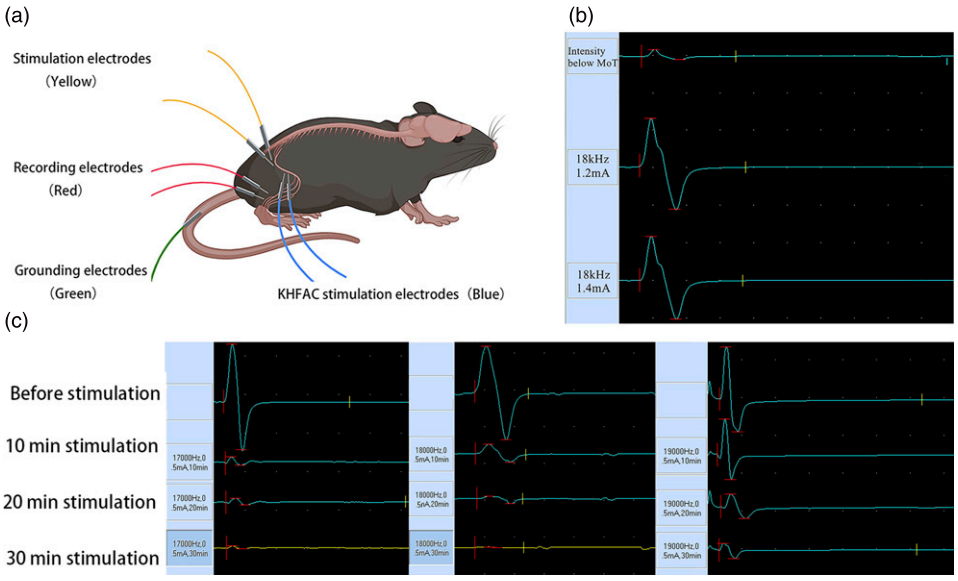

Figure 2. Electrodes' location on the mice. (a) The sciatic nerve MoT was determined by measuring sciatic nerve CMAP before high-frequency electrical stimulation. (b) The stimulation parameters were as follows: stimulation frequency of 17 kHz, current intensity of 0.5 mA; stimulation frequency of 18 kHz, current intensity of 0.5 mA; and stimulation frequency of 19 kHz, current intensity of 0.5 mA. After 30 min of KHES stimulation, the amplitude of the CMAP decreased by over 90% (c).

these findings, we performed immunofluorescence assays to detect the expression and activation of TRPV1 and NMDAR2B in the spinal cord. There were no significant differences in the activation of TRPV1 and NMDAR2B between the Sham group and the Sham/KHES group (Figure 5(g)–(j)). In contrast, the activation of TRPV1 and NMDAR2B were significantly upregulated in the CCI group (Figure 5(g)–(j), $p < .001$ for TRPV1; $p < .01$ for NMDAR2B). However, KHES treatment significantly inhibited the activation and mRNA expression of TRPV1 and NMDAR2B in the CCI/KHES group compared to the CCI group (Figure 5(g)–(j), $p < .001$ for TRPV1; $p < .01$ for NMDAR2B).

Kilohertz high frequency electrical stimulation inhibited glial cell activation in the spinal cord

The activation levels of microglia and astrocytes were reported to respond to the TRPV1/NMDAR2B pathway and inflammation levels. Therefore, we measured the expression of IBA-1 and GFAP in the spinal cord. We first detected the levels of the microglia-labeled protein IBA-1 and the astroglia-labeled protein GFAP in the spinal cord using the Western blot assay. Compared to the sham group, the expression of IBA-1 and GFAP significantly increased in the CCI group (Figure 6(a)–(d), $p < .05$ for IBA-1; $p < .0001$ for GFAP). However, KHES was able to effectively reverse the increased expression of IBA-1 and GFAP (Figure 6(a)–(d), $p < .05$ for IBA-1; $p < .001$ for GFAP). The Sham/KHES group did not show any significant changes in the protein expression of IBA-1 and GFAP compared to the Sham group (Figure 6(a)–(d)). We also detected the mRNA contents of microglia and astroglia in the spinal cord using QPCR. Our results showed that KHES was able to reduce the mRNA contents of these cell types in CCI mice (Figure 6(e)–(f), $p < .0001$ for IBA-1; $p < .0001$ for GFAP). Furthermore, we observed the morphological and quantity changes of astrocytes and microglia using immunofluorescence. Our results showed that both IBA-1 and GFAP were activated in the spinal cords of CCI model mice (Figure 6(g)–(j), $p < .05$ for IBA-1; $p < .01$ for GFAP). However, they were inhibited after high-frequency electrical stimulation, confirming that KHES inhibited the activation of microglia and astroglia in the spinal cord (Figure 6(g)–(j), $p < .01$ for IBA-1; $p < .01$ for GFAP).

Effects of transient receptor potential vanilloid-1 pathway activators and inhibitors on chronic constriction injury-induced allodynia

To further investigate the role of the TRPV1 pathway in treating CCI-induced neuropathic pain by KHES, we used TRPV1 activators and inhibitors in CCI mice. We observed the changes in pain thresholds and protein levels of mice. The TRPV1 activator capsaicin was administered intraperitoneally at a concentration of 10 mg/kg on Day 7. KHES stimulation increased the PWT (Figure 7(a), $p < .01$ from Day 8 to Day 12; $p < .001$ on Day 13) and TWL (Figure 7(b), $p < .01$ on Day 9 and Day 11; $p < .05$ on Day 10, Day 12, and Day 13) compared to the CCI + Veh group. However, the CCI + capsaicin + KHES group showed a significant reduction in PWT (Figure 7(a), $p < .05$ from

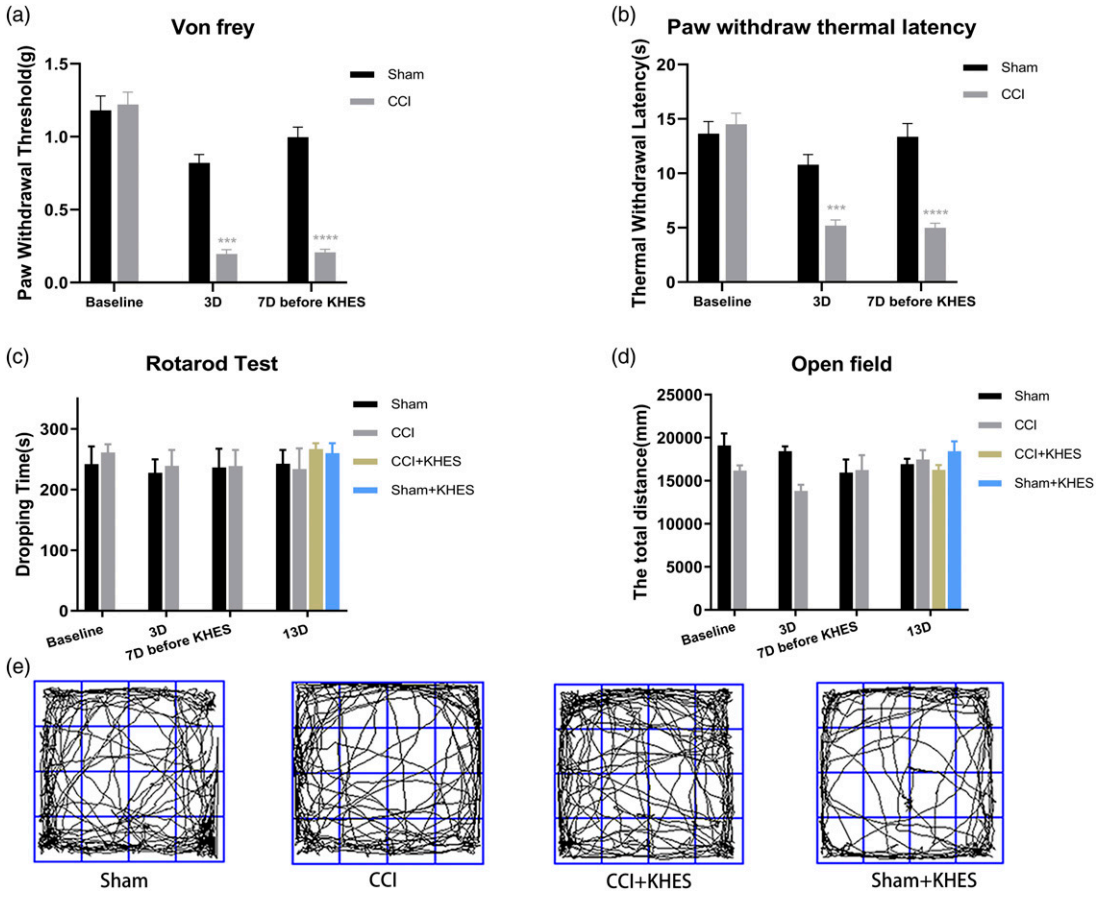

Figure 3. Behavior test of mice and motor function before and after modeling. PWT(a) and TWL(b) of the CCI group mice were significantly lower than those of sham group mice on day 3 and day 7 before KHES. There was no significant change in the dropping time in the rotarod test of the four groups before and after electrical stimulation (c). There was no significant change in the total distance in the open-field test of the four groups before and after electrical stimulation (d). Motion trajectory of open field test after KHES stimulation on Day 13 (e). ***$p < .001$, ****$p < .0001$, versus the Sham group.

Day 8 to Day 12; $p < .01$ on Day 13) and TWL (Figure 7(b), $p < .05$ from Day 9 to Day 13) compared to the CCI + Veh + KHES group. Western blotting revealed that the expressions of TRPV1 and IBA-1 were increased in the CCI + capsaicin + KHES group in contrast to the CCI + VEH + KHES group (Figure 7(c)–(f), $p < .05$ for TRPV1; $p < .05$ for IBA-1). We also administered the TRPV1 inhibitor SB-705498 at a concentration of 10 mg/kg po on Day 7. We found that SB-705498 significantly increased the PWT (Figure 7(g), $p < .05$ from Day 9 to Day 13) and TWL (Figure 7(h), p < .05 from Day 10 to Day 11; $p < .001$ on Day 12; $p < .01$ on Day 13) compared to the CCI + VEH group. However, there was no significant difference in pain threshold between the CCI + SB-705498 group and the CCI + VEH + KHES group. Western blotting analysis revealed that the expressions of TRPV1 and IBA-1 in the CCI + SB-705498 group were significantly decreased compared to the CCI + VEH group (Figure 7(i–l), $p < .01$ for TRPV1; $p < .01$ for IBA-1), but there was no striking difference between the CCI + SB-705498 group and the CCI + VEH + KHES group.

Discussion

Neuropathic pain is a challenging and complicated disorder that poses significant difficulties in terms of treatment.[34] Despite the availability of various drugs, these medications are only effective in managing general neuropathic pain. Several clinical trials have demonstrated that tricyclic antidepressants can only provide pain control in around 30% of cases and are often associated with common anticholinergic adverse reactions, including sedation, dry mouth, and constipation.[35] Therefore, there is a need for non-invasive neuromodulation methods that can effectively treat neuropathic pain while minimizing the incidence of adverse reactions. In this regard, we suggest the use of KHES as a promising alternative to conventional drug-based treatments. Our study shows that KHES was able to significantly reduce

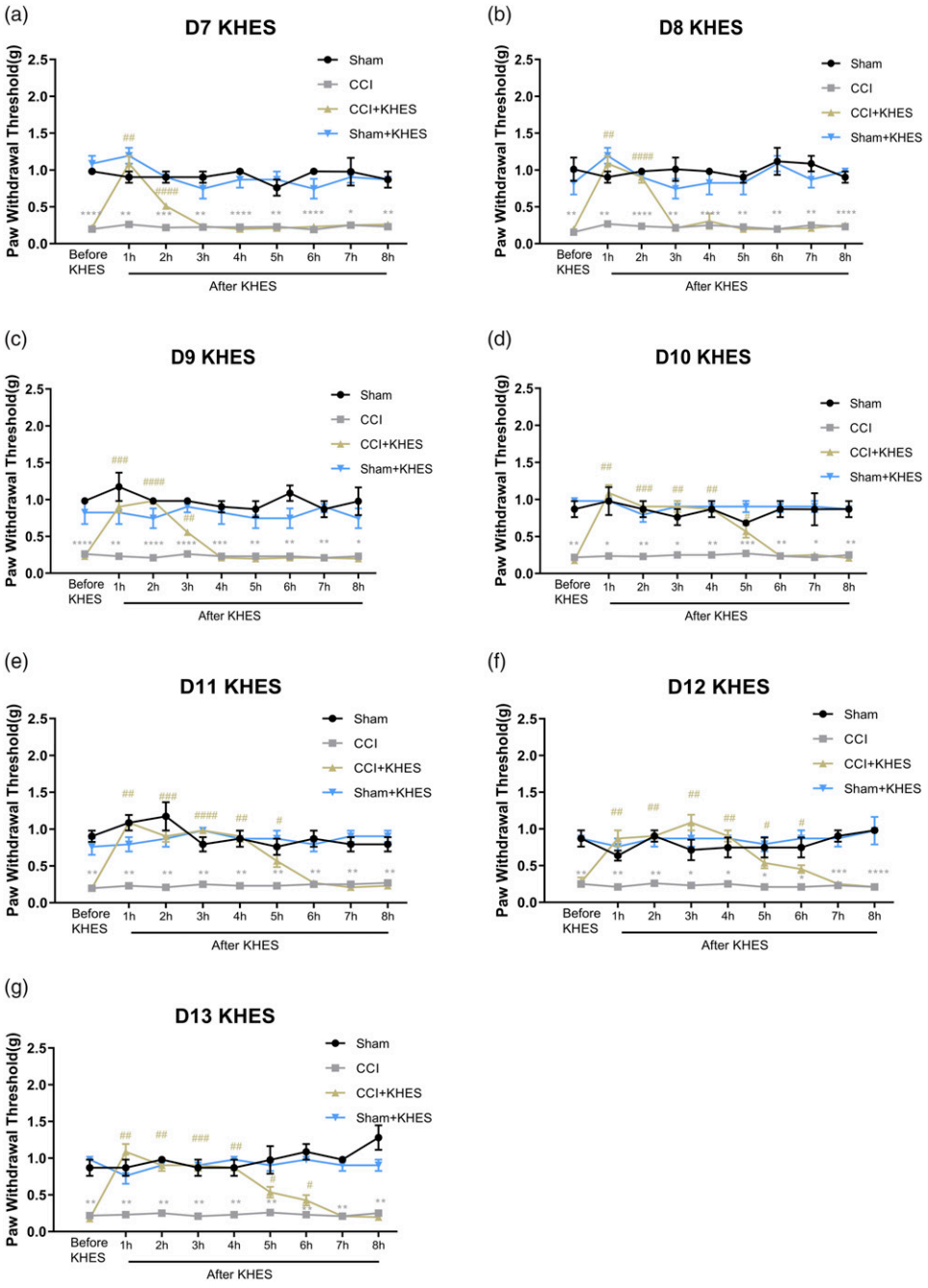

Figure 4. Changes of mechanical pain threshold in four groups after KHES stimulation. KHES alleviated the mechanical pain for 2h, 2h, 3h, 5h, 5h, 6h, and 6h from day 7 to day 13. *$p < .05$, **$p < .01$, ***$p < .001$, ****$p < .0001$ versus the Sham group; $^{\#}p < .05$, $^{\#\#}p < .01$, $^{\#\#\#}p < .001$, $^{\#\#\#\#}p < .0001$ versus the CCI group.

mechanical and thermal allodynia in mice with CCI-induced neuropathic pain. Additionally, we explored the relationship between KHES and the TRPV1/NMDAR2B pathway, shedding light on the mechanisms underlying the effectiveness of KHES in treating neuropathic pain. These findings highlight the potential of KHES as a safe, effective, and non-invasive therapy for neuropathic pain.

Low-frequency electrical stimulation has been found to elicit analgesic effects through the activation of spinal dorsal column axons, effectively inhibiting the transmission of pain information carried by wide dynamic range (WDR) neurons.[36] However, it is worth noting that this stimulation can also stimulate large-diameter fibers responsible for conveying vibration sensations, resulting in a sensation of paralysis.

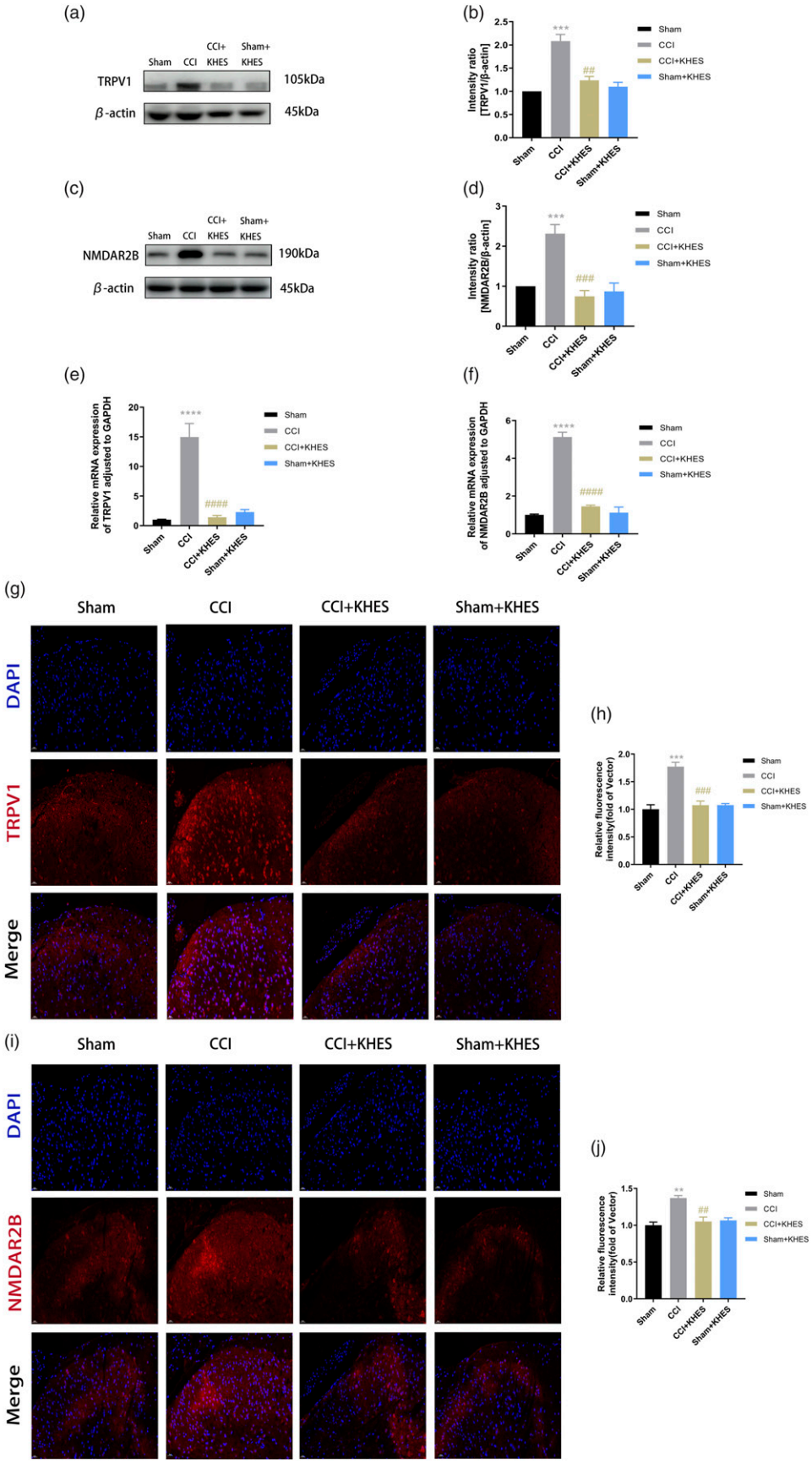

Figure 5. Expression of TRPV1 and NMDAR2B in the spinal cord after KHES-inhibited postoperative hyperalgesia. Western blot of TRPV1 and NMDAR2B expressions in operative L4 – L6 spinal cord. (a–d) The mRNA levels of TRPV1 and NMDAR2B in the spinal cord were detected by QPCR. (e–f) Immunohistochemical analyses and statistical histogram of the immunofluorescence of TRPV1 and NMDAR2B immunoreactive positive neurons. Scale bar = 20 μm. (g–j) All the results were expressed as mean ± SEM and analyzed by one-way ANOVA followed by Tukey's post hoc tests. $^{**}p < .01$, $^{***}p < .001$, $^{****}p < .0001$versus the Sham group; $^{\#\#}p < .01$, $^{\#\#\#}p < .001$, $^{\#\#\#\#}p < .0001$ versus the CCI group.

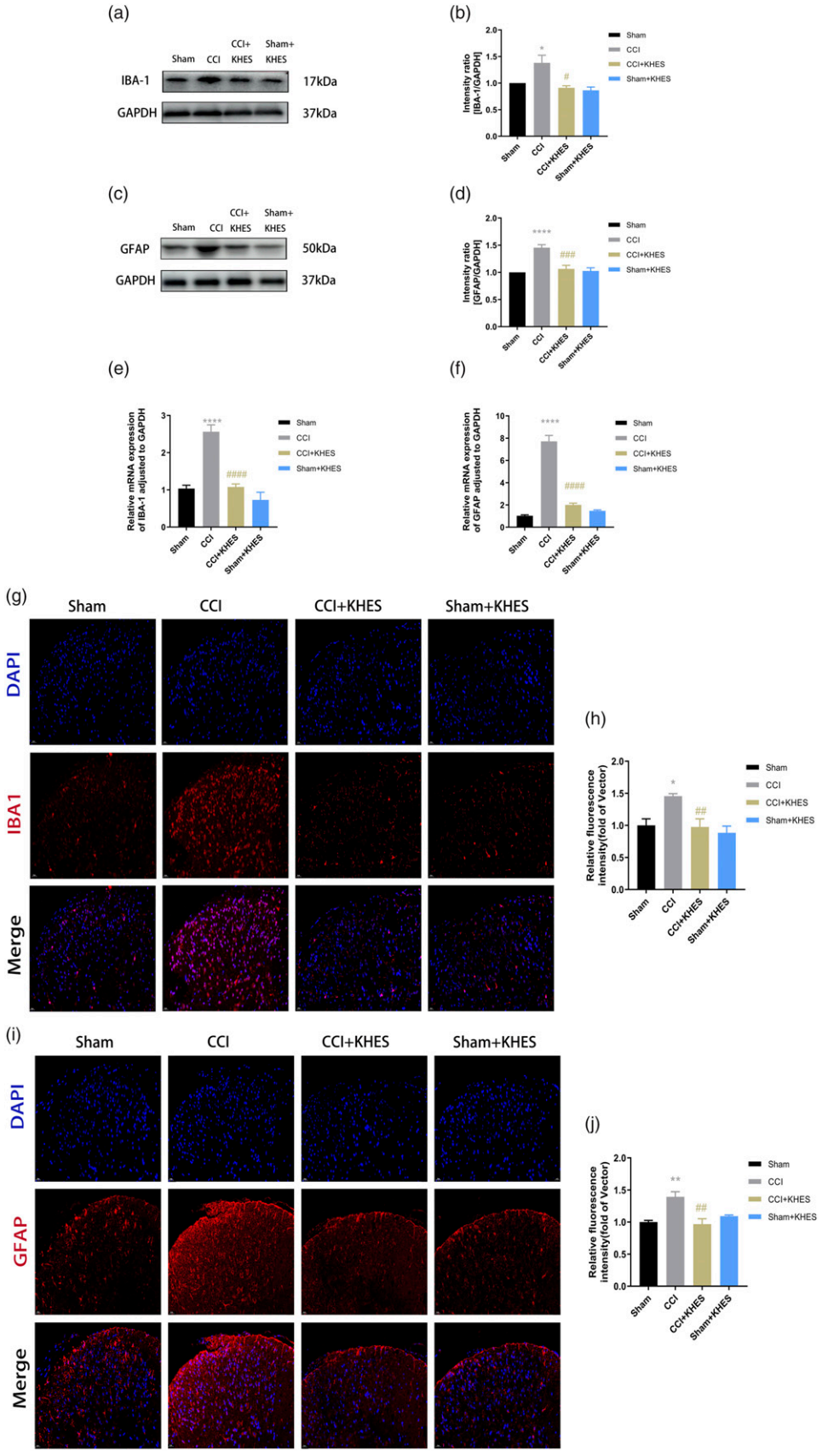

Figure 6. Expression of IBA-1 and GFAP in the spinal cord after KHES stimulation. Western blot of IBA-1 and GFAP expressions in operative L4 – L6 spinal cord. (a–d) The mRNA levels of IBA-1 and GFAP in the spinal cord were detected by QPCR. (e–f) Immunohistochemical analyses and statistical histogram of the immunofluorescence of IBA-1 and GFAP immunoreactive positive neurons. Scale bar = 20 μm. (g–j) All the results were expressed as mean ± SEM and analyzed by one-way ANOVA followed by Tukey's post hoc tests. *$p < .05$, **$p < .01$, ****$p < .0001$ versus Sham group; ##$p < .01$, $^{###}p < .001$, $^{####}p < .0001$ versus the CCI group.

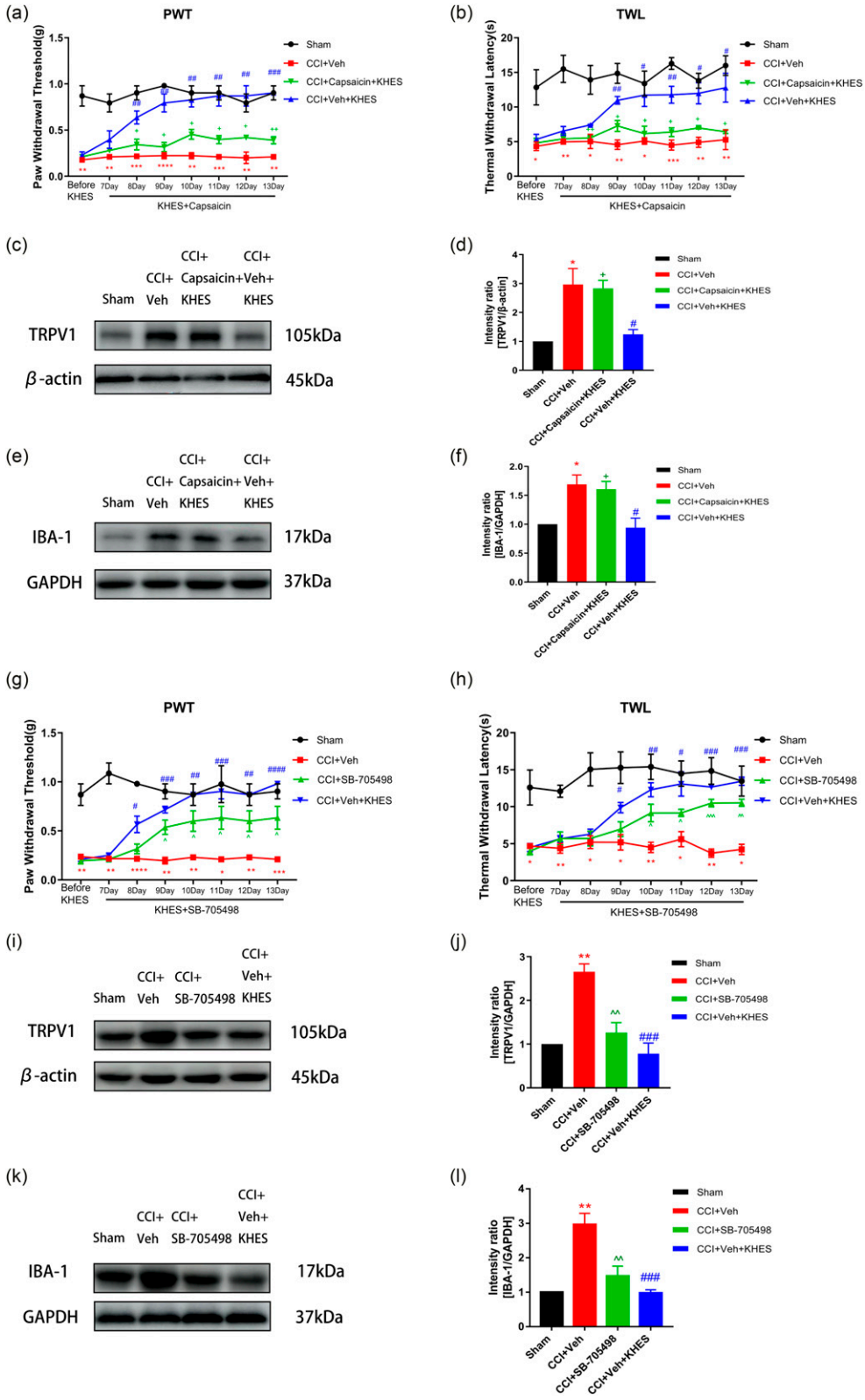

Figure 7. The effects of TRPV1 pathway activators and inhibitors on CCI-induced allodynia. The administration of TRPV1 pathway activator capsaicin (10 mg/kg) partially reversed the antinociceptive effects of KHES on mechanical and thermal pain from day 8 to day 13. (a–b) Western blotting showed the expression of TRPV1 and IBA-1. (c-f) The TRPV1 pathway inhibitor SB-705498 (10 mg/kg) reversed the antinociceptive of KHES on mechanical and thermal pain from day 9 to day 13. (g-h) Western blotting showed the expression of SB-705498 in four groups. (i–l) $^{\#}p < .05$, $^{\#\#}p < .01$, $^{\#\#\#}p < .001$ versus the CCI + Veh group; $^{+}p < .05$, $^{++}p < .01$ versus the CCI + Veh + KHES group; $\hat{}p < .05$, $\hat{}\hat{}p < .01$, $\hat{}\hat{}\hat{}p < .001$ versus the CCI + Veh group.

Regarding the phenomenon that KHES does not cause a sense of paralysis but alleviates pain, a reasonable hypothesis has been proposed: KHES can selectively block the large fibers involved in vibration sensation while simultaneously activating medium and small-diameter fibers that do not elicit a sense of paralysis. Once a sufficient number of these medium and small-diameter fibers are activated, they can effectively suppress the pain transmission by WDR cells, thereby achieving analgesic effects.[37] In comparison to the conventional low-frequency electrical stimulation, KHES exhibits greater efficacy in reducing the severity of chronic back and leg pain in patients, and it boasts a wider range of applications.[38] Moreover, in a separate experiment, neuropathologic pain rats demonstrated enhanced motor nerve regeneration and improved potential following KHES treatment.[39] Nonetheless, recent study suggests that using a high-frequency carrier does not improve comfort of transcutaneous spinal cord stimulation. The higher stimulation charge needed to evoke a response with the high-frequency carrier waveform requires the stimulator to produce much higher voltages, increasing the power budget and risk of injury.[40] The stimulation current employed in our study was 0.5 mA. Given the proximity of the stimulation electrode to the sciatic nerve, the requisite stimulation charge is relatively modest, thereby minimizing the likelihood of discomfort. However, additional clinical experiments are warranted to explore any potential occurrence of abnormal sensations in patients as a result of the KHES stimulation method and parameters.

It is worth noting that KHES stimulation initially leads to a brief but intense neural activity, commonly referred to as the onset response.[41] To address this issue, a study conducted by T L Vrabec et al. on rats' sciatic nerves demonstrated that implementing subthreshold ramping can effectively prevent the onset response during prolonged KHES block following the initial onset. It has been observed that amplitudes exceeding 50% of the block threshold can be safely ramped up to 125% without any onset occurrence, while amplitudes below 25% will consistently result in an onset. Increasing the subthreshold percentage decreases the minimum ramp time required to produce an onset. Furthermore, the study observed that subthreshold amplitudes set at 50% of the block threshold demonstrate a nearly complete absence of block. This suggests that the block can be activated or deactivated independently, even when KHES is continuously active, offering a potential approach to maintaining a no-onset KHES block.[42] Thomas Eggers et al. have proposed a novel waveform that combines direct current and kilohertz frequency alternating current to initiate block without onset response and maintain safe block for extended periods. Their approach involves using direct current to initiate the block and rapidly switching to kilohertz frequency alternating current to sustain the block with minimal onset response during the transition. The amplitude and duration of the direct current portion of the waveform are personalized during stimulation to determine the optimal values for reducing onset responses.[43] By minimizing or eliminating the onset response, these approaches could potentially improve patient tolerance and acceptance of KHES as a non-invasive neuromodulation method for neuropathic pain management.

In our previous study, we conducted a comprehensive analysis using the publicly available GEO database of gene expression data to identify suitable datasets related to neuropathic pain in mice. Through KEGG pathway analysis, we identified glutamatergic synapses and TRP channels, specifically the ion channels involved in sensory transduction, as potential pathways associated with the development of neuropathic pain.[8] Building upon these findings, our current research has confirmed the upregulation of TRPV1 and NMDAR2B expression in the spinal cord of neuropathic pain mice following CCI modeling, and KHES has significantly reversed the increasing trend of TRPV1 and NMDAR2B expression. Despite this progress, the functional relationship between TRPV1 and NMDA receptors in neuropathic pain regulation remains poorly understood. Jongseok Lee et al. demonstrated that NMDA receptors and TRPV1 form functional complexes through Ca2 + calmodulin-dependent protein kinase II (CaMKII) and protein kinase C (PKC) signaling cascades, contributing to the development of mechanical hyperalgesia in the masseter muscle of rats.[44] Additionally, another study reported that ginger extract and its compound, 6-shogaol, alleviate painful diabetic neuropathy in mice by reducing TRPV1 and NMDAR2B expression in the spinal cord.[45] These findings align with the interactions between TRPV1 and NMDA receptors in the mouse spinal cord. In our investigation, we observed a notable inhibition of GFAP and IBA1 expression in the spinal cord following treatment with KHES. Furthermore, inhibitors and activators of the TRPV1 channel affected pain thresholds and the expression of spinal cord IBA1 in neuropathic pain mice. It is now widely recognized that the pathogenesis of neuropathic pain involves not only alterations in neuronal system activity but also intricate interactions between neurons, inflammatory immune cells, and immune-like glial cells.[46] While neuroinflammation serves as a beneficial process in promoting regeneration and healing under physiological conditions, its persistent presence is thought to contribute to the development of neuropathic pain.[47–49] Based on our findings, we propose that KHES exerts its therapeutic effects on neuropathic pain by modulating inflammatory factors, including GFAP and IBA1, within the spinal cord via the TRPV1/NMDAR2B signaling pathway.

Our research has several noteworthy limitations. Firstly, our analysis relied on publicly available databases, which may introduce some degree of bias and limit the generalizability of our findings. To address this limitation and gain a more comprehensive understanding of the mechanisms underlying the analgesic effects of KHES, future studies could incorporate sample collection from each group of mice following KHES intervention and perform transcriptomic sequencing to explore potential pathways and gene expression changes in a more targeted manner. Another limitation of our

study is the exclusive focus on male mice, which may overlook potential gender differences in the response to KHES treatment. Previous studies have demonstrated that immune cell-mediated mechanical hypersensitivity responses can differ between male and female mice.[50] Therefore, it would be valuable to include an equal number of female mice in future experiments to assess whether the analgesic effects and underlying mechanisms of KHES vary between genders. It is important to note that our study represents an early stage of research in this field, and further investigations are warranted to build upon our findings. While our study did not directly demonstrate a causal relationship between the TRPV1/NMDAR2B pathway and the activation of glial cells, our results indicate that the modulation of this pathway by KHES may play a role in inhibiting glial cell activation, suggesting a potential association between these factors. We acknowledge the need for further studies to establish a direct causal relationship and understand the precise mechanisms underlying the inhibitory effects of KHES on glial cell activation. To address this limitation, we plan to employ advanced techniques such as transcriptome sequencing and patch-clamp recordings to further investigate the impact of KHES on the expression and function of NR2B and TRPV1 channels. Future studies could explore additional molecular and cellular mechanisms, conduct behavioral assessments with a more comprehensive battery of pain tests, and evaluate the long-term effects and safety profile of KHES treatment. By addressing these limitations, future research can provide a more robust understanding of the potential therapeutic applications of KHES for neuropathic pain management.

Conclusion

Our study has shown that the analgesic duration of the CCI model mice increased as the number of days of high-frequency electrical stimulation increased, up to 6 h. We found that KHES affected the activation of glial cells in the spinal cord by inhibiting the expression of TRPV1 and NMDAR2B, thereby improving neuropathic pain. Our results also revealed that the antinociceptive effect of KHES could be partially reversed by the activation of the TRPV1 pathway, which was accompanied by a suppression of microglial activation. Conversely, the use of TRPV1 pathway antagonist produced a similar analgesic effect. Therefore, KHES could be a promising new treatment for neuropathic pain. Future studies should focus on conducting clinical trials to assess the effectiveness of KHES in human patients and investigate additional pathways and molecular targets that may contribute to its therapeutic effects.

Appendix

Abbreviations

KHES	Kilohertz high frequency electrical stimulation
GEO	Gene expression omnibus
TRPV1	Transient receptor potential vanilloid-1
NMDAR2B	N-methyl-D-aspartate receptor-2B
CCI	Chronic constriction injury
PWT	Paw withdrawal threshold
TWL	Thermal withdrawal latency
GFAP	Glial fibrillary acidic protein
IBA1	Ionized calcium binding adapter molecule one
KEGG	Kyoto encyclopedia of genes and genomes
NF-KB	Nuclear factor KB
TRP	Transient receptor potential
cAMP	Cyclic adenosine monophosphate
Myd88	Myeloid differentiation factor 88
NMDA	N-methyl-D-aspartate
MoT	Motor threshold
SenT	Sensory threshold
CMAP	Compound muscle action potential
CaMKII	Calmodulin-dependent protein kinase II
PKC	Protein kinase C.

Acknowledgements

We want to express our sincere gratitude to Yangzhi Affiliated Rehabilitation Hospital, Tongji University and Shanghai Tongji Hospital for providing the laboratory and equipment.

Author contributions

Bin Yu and Kexin Fang concepted and designed this study. Kexin Fang and Wen Cheng performed the research and analyzed the results. Peixin Lu helped Kexin Fang write the manuscript and prepare the figures and tables. All authors agree on the journal to which the article has been submitted and claim no conflicts of interest.

Declaration of conflicting interests

The author(s) declared no potential conflicts of interest with respect to the research, authorship, and/or publication of this article.

Funding

The author(s) disclosed receipt of the following financial support for the research, authorship, and/or publication of this article: This work was supported by the National Natural Science Foundation of China, Grant No. 81974167.

Ethical statement

Ethical approval

The datasets analyzed during the current study are available from the corresponding author upon reasonable request. All experiments adhered to the National Institutes of Health (NIH) Guide for the Care and Use of Laboratory Animals. The study was approved by Shanghai Tongji Hospital Animal Ethics Committee.

ORCID iD

Bin Yu https://orcid.org/0000-0002-7218-7535

Supplemental Material

Supplemental material for this article is available online.

References

1. Horowitz SH. Response to commentary: a new definition of neuropathic pain. *Pain* 2012; 153: 935.
2. Bouhassira D, Lantéri-Minet M, Attal N, Laurent B, Touboul C. Prevalence of chronic pain with neuropathic characteristics in the general population. *Pain* 2008; 136: 380–387.
3. Gilron I, Baron R, Jensen T. Neuropathic pain: principles of diagnosis and treatment. *Mayo Clin Proc* 2015; 90: 532–545.
4. von Hehn CA, Baron R, Woolf CJ. Deconstructing the neuropathic pain phenotype to reveal neural mechanisms. *Neuron* 2012; 73: 638–652.
5. Kilgore KL, Bhadra N. Reversible nerve conduction block using kilohertz frequency alternating current. *Neuromodulation* 2014; 17: 242–255.
6. Roldan LM, Eggers TE, Kilgore KL, Bhadra N, Vrabec T, Bhadra N. Measurement of block thresholds in kiloHertz frequency alternating current peripheral nerve block. *J Neurosci Methods* 2019; 315: 48–54.
7. Cogan SF. Neural stimulation and recording electrodes. *Annu Rev Biomed Eng* 2008; 10: 275–309.
8. Lu P, Fang K, Cheng W, Yu B. High-frequency electrical stimulation reduced hyperalgesia and the activation of the Myd88 and NFκB pathways in chronic constriction injury of sciatic nerve-induced neuropathic pain mice. *Neurosci Lett* 2023; 796: 137064.
9. Gaunitz C, Schüttler A, Gillen C, Allgaier C. Formalin-induced changes of NMDA receptor subunit expression in the spinal cord of the rat. *Amino Acids* 2002; 23: 177–182.
10. Shigemoto R, Ohishi H, Nakanishi S, Mizuno N. Expression of the mRNA for the rat NMDA receptor (NMDAR1) in the sensory and autonomic ganglion neurons. *Neurosci Lett* 1992; 144: 229–232.
11. Carpenter KJ, Dickenson AH. NMDA receptors and pain–hopes for novel analgesics. *Reg Anesth Pain Med* 1999; 24: 506–508.
12. Li L, Wu Y, Bai Z, Hu Y, Li W. Blockade of NMDA receptors decreased spinal microglia activation in bee venom induced acute inflammatory pain in rats. *Neurol Res* 2017; 39: 271–280.
13. Chen Y, Geis C, Sommer C. Activation of TRPV1 contributes to morphine tolerance: involvement of the mitogen-activated protein kinase signaling pathway. *J Neurosci* 2008; 28: 5836–5845.
14. Abooj M, Bishnoi M, Bosgraaf CA, Premkumar LS. Changes in spinal cord following inflammatory and neuropathic pain and the effectiveness of resiniferatoxin. *Open Pain J* 2016; 9: 1–14.
15. Caterina MJ, Schumacher MA, Tominaga M, Rosen TA, Levine JD, Julius D. The capsaicin receptor: a heat-activated ion channel in the pain pathway. *Nature* 1997; 389: 816–824.
16. Ji RR, Samad TA, Jin SX, Schmoll R, Woolf CJ. p38 MAPK activation by NGF in primary sensory neurons after inflammation increases TRPV1 levels and maintains heat hyperalgesia. *Neuron* 2002; 36: 57–68.
17. Alawi K, Keeble J. The paradoxical role of the transient receptor potential vanilloid 1 receptor in inflammation. *Pharmacol Ther* 2010; 125: 181–195.
18. Shin YH, Kim JM, Park K. The effect of capsaicin on salivary gland dysfunction. *Molecules* 2016; 21: 835.
19. Caterina MJ, Julius D. The vanilloid receptor: a molecular gateway to the pain pathway. *Annu Rev Neurosci* 2001; 24: 487–517.
20. Gunthorpe MJ, Rami HK, Jerman JC, Smart D, Gill CH, Soffin EM, Luis Hannan S, Lappin SC, Egerton J, Smith GD, Worby A, Howett L, Owen D, Nasir S, Davies CH, Thompson M, Wyman PA, Randall AD, Davis JB. Identification and characterisation of SB-366791, a potent and selective vanilloid receptor (VR1/TRPV1) antagonist. *Neuropharmacology* 2004; 46: 133–149.
21. Gunthorpe MJ, Hannan SL, Smart D, Jerman JC, Arpino S, Smith GD, Brough S, Wright J, Egerton J, Lappin SC, Holland VA, Winborn K, Thompson M, Rami HK, Randall A, Davis JB. Characterization of SB-705498, a potent and selective vanilloid receptor-1 (VR1/TRPV1) antagonist that inhibits the capsaicin-, acid-, and heat-mediated activation of the receptor. *J Pharmacol Exp Therapeut* 2007; 321: 1183–1192.
22. Song C, Liu P, Zhao Q, Guo S, Wang G. TRPV1 channel contributes to remifentanil-induced postoperative hyperalgesia via regulation of NMDA receptor trafficking in dorsal root ganglion. *J Pain Res* 2019; 12: 667–677.
23. Yao CY, Weng ZL, Zhang JC, Feng T, Lin Y, Yao S. Interleukin-17A acts to maintain neuropathic pain through activation of CaMKII/CREB signaling in spinal neurons. *Mol Neurobiol* 2016; 53: 3914–3926.
24. Crown ED, Gwak YS, Ye Z, Yu Tan H, Johnson KM, Xu GY, McAdoo DJ, Hulsebosch CE. Calcium/calmodulin dependent kinase II contributes to persistent central neuropathic pain following spinal cord injury. *Pain* 2012; 153: 710–721.
25. Mosconi T, Kruger L. Fixed-diameter polyethylene cuffs applied to the rat sciatic nerve induce a painful neuropathy: ultrastructural morphometric analysis of axonal alterations. *Pain* 1996; 64: 37–57.
26. Pitcher GM, Ritchie J, Henry JL. Nerve constriction in the rat: model of neuropathic, surgical and central pain. *Pain* 1999; 83: 37–46.
27. Meyerson BA, Linderoth B. Mode of action of spinal cord stimulation in neuropathic pain. *J Pain Symptom Manag* 2006; 31: S6–S12.
28. Song Z, Ultenius C, Meyerson BA, Linderoth B. Pain relief by spinal cord stimulation involves serotonergic mechanisms: an experimental study in a rat model of mononeuropathy. *Pain* 2009; 147: 241–248.
29. Shechter R, Yang F, Xu Q, Cheong YK, He SQ, Sdrulla A, Carteret AF, Wacnik PW, Dong X, Meyer RA, Raja SN, Guan Y. Conventional and kilohertz-frequency spinal cord stimulation produces intensity- and frequency-dependent inhibition of

mechanical hypersensitivity in a rat model of neuropathic pain. *Anesthesiology* 2013; 119: 422–432.
30. Cattell M, Gerard RW. The "inhibitory"| effect of high-frequency stimulation and the excitation state of nerve. *J Physiol* 1935; 83: 407–415.
31. Hargreaves K, Dubner R, Brown F, Flores C, Joris J. A new and sensitive method for measuring thermal nociception in cutaneous hyperalgesia. *Pain* 1988; 32: 77–88.
32. Anandakumar P, Kamaraj S, Jagan S, Ramakrishnan G, Devaki T. Capsaicin provokes apoptosis and restricts benzo(a)pyrene induced lung tumorigenesis in Swiss albino mice. *Int Immunopharm* 2013; 17: 254–259.
33. Rami HK, Thompson M, Stemp G, Fell S, Jerman JC, Stevens AJ, Smart D, Sargent B, Sanderson D, Randall AD, Gunthorpe MJ, Davis JB. Discovery of SB-705498: a potent, selective and orally bioavailable TRPV1 antagonist suitable for clinical development. *Bioorg Med Chem Lett* 2006; 16: 3287–3291.
34. Finnerup NB, Kuner R, Jensen TS. Neuropathic pain: from mechanisms to treatment. *Physiol Rev* 2021; 101: 259–301.
35. Cruccu G, Sommer C, Anand P, Attal N, Baron R, Garcia-Larrea L, Haanpaa M, Jensen TS, Serra J, Treede RD. EFNS guidelines on neuropathic pain assessment: revised 2009. *Eur J Neurol* 2010; 17: 1010–1018.
36. Linderoth B, Meyerson BA. Spinal cord stimulation: exploration of the physiological basis of a widely used therapy. *Anesthesiology* 2010; 113: 1265–1267.
37. Arle JE, Mei L, Carlson KW, Shils JL. High-frequency stimulation of dorsal column axons: potential underlying mechanism of paresthesia-free neuropathic pain relief. *Neuromodulation* 2016; 19: 385–397.
38. Kapural L, Yu C, Doust MW, Gliner BE, Vallejo R, Sitzman BT, Amirdelfan K, Morgan DM, Yearwood TL, Bundschu R, Yang T, Benyamin R, Burgher AH. Comparison of 10-kHz high-frequency and traditional low-frequency spinal cord stimulation for the treatment of chronic back and leg pain: 24-month results from a multicenter, randomized, controlled pivotal trial. *Neurosurgery* 2016; 79: 667–677.
39. Su HL, Chiang CY, Lu ZH, Cheng FC, Chen CJ, Sheu ML, Sheehan J, Pan HC. Late administration of high-frequency electrical stimulation increases nerve regeneration without aggravating neuropathic pain in a nerve crush injury. *BMC Neurosci* 2018; 19: 37.
40. Dalrymple AN, Hooper CA, Kuriakose MG, Capogrosso M, Weber DJ. Using a high-frequency carrier does not improve comfort of transcutaneous spinal cord stimulation. *J Neural Eng* 2023; 20. DOI: 10.1088/1741-2552/acabe8
41. Bhadra N, Bhadra N, Kilgore K, Gustafson KJ. High frequency electrical conduction block of the pudendal nerve. *J Neural Eng* 2006; 3: 180–187.
42. Vrabec TL, Eggers TE, Foldes EL, Ackermann DM, Kilgore KL, Bhadra N. Reduction of the onset response in kilohertz frequency alternating current nerve block with amplitude ramps from non-zero amplitudes. *J NeuroEng Rehabil* 2019; 16: 80.
43. Eggers T, Kilgore J, Green D, Vrabec T, Kilgore K, Bhadra N. Combining direct current and kilohertz frequency alternating current to mitigate onset activity during electrical nerve block. *J Neural Eng*. 2021; 18: 10. doi:10.1088/1741-2552/abebed
44. Lee J, Saloman JL, Weiland G, Auh QS, Chung MK, Ro JY. Functional interactions between NMDA receptors and TRPV1 in trigeminal sensory neurons mediate mechanical hyperalgesia in the rat masseter muscle. *Pain* 2012; 153: 1514–1524.
45. Fajrin FA, Nugroho AE, Nurrochmad A, Susilowati R. Ginger extract and its compound, 6-shogaol, attenuates painful diabetic neuropathy in mice via reducing TRPV1 and NMDAR2B expressions in the spinal cord. *J Ethnopharmacol* 2020; 249: 112396.
46. Austin PJ, Moalem-Taylor G. The neuro-immune balance in neuropathic pain: involvement of inflammatory immune cells, immune-like glial cells and cytokines. *J Neuroimmunol* 2010; 229: 26–50.
47. Huh Y, Ji RR, Chen G. Neuroinflammation, bone marrow stem cells, and chronic pain. *Front Immunol* 2017; 8: 1014.
48. Ji RR, Chamessian A, Zhang YQ. Pain regulation by non-neuronal cells and inflammation. *Science* 2016; 354: 572–577.
49. Littlejohn G. Neurogenic neuroinflammation in fibromyalgia and complex regional pain syndrome. *Nat Rev Rheumatol* 2015; 11: 639–648.
50. Sorge RE, Mapplebeck JC, Rosen S, Beggs S, Taves S, Alexander JK, Martin LJ, Austin JS, Sotocinal SG, Chen D, Yang M, Shi XQ, Huang H, Pillon NJ, Bilan PJ, Tu Y, Klip A, Ji RR, Zhang J, Salter MW, Mogil JS. Different immune cells mediate mechanical pain hypersensitivity in male and female mice. *Nat Neurosci* 2015; 18: 1081–1083.